INSTITUTE OF PHYSICS PUBLISHING NANOTECHNOLOGY
Nanotechnology **17** (2006) 1241–1244 doi:10.1088/0957-4484/17/5/013

Three-dimensional low-index-contrast photonic crystals fabricated using a tunable beam splitter

Ivan Divliansky[1] **and Theresa S Mayer**

Department of Electrical Engineering, Center for Nanoscale Science, The Pennsylvania State University, University Park, PA 16802, USA

E-mail: tsm2@psu.edu (T Mayer)

Received 17 November 2005, in final form 3 January 2006
Published 7 February 2006
Online at stacks.iop.org/Nano/17/1241

Abstract
This paper describes the design and implementation of a tunable beam splitter for fabricating three-dimensional low-index-contrast photonic crystals using four-beam interference. Here, a central console is used to split a single laser beam into four beams that are focused onto the sample in an umbrella-like configuration using three adjustable mirrors. The design facilitates simple and precise adjustments of the beam angles and polarization, which can be used to readily optimize fabrication conditions for different photosensitive materials and lattice structures. Structures fabricated using this tunable beam splitter at two different incident angles of 18.5° and 27° resulted in lattices with hexagonal symmetries having well-defined nanometre-scale features that are in close agreement with the feature sizes predicted theoretically.

1. Introduction

Interference lithography has emerged as an important method for fabricating one-, two-, and three-dimensional (1D, 2D, and 3D) periodic or quasi-periodic patterns for a variety of applications. One of the earliest demonstrations involved forming 1D diffraction gratings with nanometre periodicity in a photosensitive polymer [1, 2]. Later, more complex 2D and 3D patterns were implemented for use in field emission displays [3] and laser cooling/trapping experiments [4, 5]. It was determined from these studies that patterns with different space symmetries including hexagonal, square, body-centred, and face-centred cubic can be generated by simply modifying the arrangement of the interfering beams [5]. More recently, Campbell *et al* introduced the use of interference lithography for fabricating low-index 3D photonic crystals (PCs) using four-beam interference [6]. A face-centred cubic structure was obtained by interference of a normally incident central beam with three additional beams oriented at 38.9° relative to the central beam. Several other groups proposed and implemented additional 3D structures including diamond PCs using a similar optical arrangement [7–10].

In this paper, we describe the design and implementation of a new tunable beam splitter that can be used to create four-beam interference patterns with different periodicities for fabricating nanometre-scale 3D PC structures. The beam splitter comprises a central console that is used to split a single laser beam into four beams that are focused onto the sample in an umbrella-like configuration using three adjustable mirrors. In contrast to previous approaches that require three or more separate beam splitters to produce the four beams [6–10], this design simplifies the optomechanical set-up by using only one beam-splitting element while still allowing the angles, intensities, and polarizations of each of the four beams to be adjusted independently. This reduces greatly the complexity of aligning the optical set-up and provides flexibility for fabricating 3D PCs with different crystal lattice constants and structures from a variety of photosensitive materials. As an example, structures produced using this tunable beam splitter by exposing commercially available, negative tone photoresist at two different incident angles of 18.5° and 27° resulted in lattices with hexagonal symmetries having well-defined nanometre-scale features.

2. Experimental methods

A schematic diagram of the tunable beam splitter is shown in figure 1. The device comprises a central console that is surrounded by three adjustable mirrors. The console is

[1] Present address: College of Optics and Photonics: CREOL & FPCE, University of Central Florida, Orlando, FL 32816, USA.

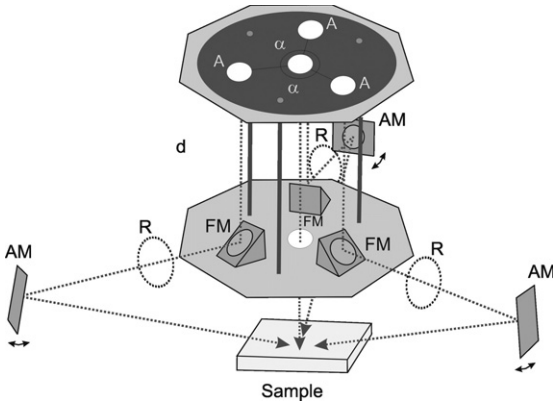

Figure 1. Tunable beam splitter design (A—apertures, FM—45° pyramids accommodating fixed mirrors, R—polarizer/analyser optics, AM—mirrors placed on rotational mounts, $\alpha = 120°$). The incident laser beam is represented by the dark circle on the top plate. The R optics used for the central beam was placed underneath the console (not shown in figure).

constructed from two parallel metal plates that are separated by a distance d. The top plate contains four circular apertures (labelled A) that are located at the corners and the centre of an equilateral triangle. Here, the apertures are used to transform a single expanded laser beam that is normally incident on the top surface of the console into four separate beams that are projected onto the bottom plate. The bottom plate has a single aperture aligned with the central aperture in the top plate, which allows the central beam to travel directly through the console and onto the sample. This plate also accommodates three fixed mirrors (labelled FM) that are centred below the remaining three apertures and oriented at 45° relative to the bottom plate. The fixed mirrors are positioned to translate the three outer beams that propagate parallel to each other from the top to bottom plates, to beams that propagate parallel to the bottom plate with an angle of 120° separating them. These three beams are returned to interfere with the central beam at precise, user-defined adjustable angles. This is accomplished using three additional mirrors (labelled AM) placed on graduated rotational mounts that are spaced equidistantly from the lower plate of the console.

Samples coated with negative tone photoresist layers are patterned in a single step by aligning them in the focal plane of the four interfering beams (labelled *Sample*). The position of the focal plane depends on the incident angle of the outer beams relative to sample surface and on the distance between the adjustable mirrors and the console. Because the beam distribution is localized to the region above the sample, exposures can be made on opaque as well as transparent substrates. However, it should be noted that an antireflection coating must be applied to the surface of opaque substrates to prevent back-reflections that can have an impact on the interference pattern.

It has been shown previously that the relative polarization and the intensity of each of the beams are key factors in producing interference patterns with high contrast [11–13], which is necessary for achieving well-defined open 3D patterns and structures. The tunable beam splitter design described here provides ample space and flexibility to include additional optics such as polarizers and analysers (labelled R) for precisely adjusting the individual beam polarizations and intensities in the different beam paths; the location of the R optics between the fixed and adjustable mirrors (FM and AM) simplifies alignment and adjustment of these optical elements.

The remainder of the optical set-up is similar to that reported in [14]. In the experiments described here, we used the 351 nm line of a Coherent Innova 300-Series Ar^+ continuous-wave (CW) laser as the exposure source. The 1.5 mm laser beam was expanded to a final diameter of approximately 30 mm, which completely covers the top plate (and corresponding apertures) of the console. A horizontal beam polarization was maintained for all of the experiments. The Gaussian distribution of the expanded beam resulted in slight differences in intensity of the central and outer beams. Thus, an additional polarizer was inserted underneath the console to adjust the intensity of the central beam to equal that of the three outer beams.

The 3D patterns were recorded in a negative tone, i-line photoresist (NR5-8000, Futurrex, Inc). This resist was selected because it has excellent resolution, can be spun to thicknesses of 120 μm, requires a short single-step soft bake, and is soluble for use in solvents such as acetone and isopropyl or ethyl alcohols. These properties offer advantages over alternative negative tone resists such as SU-8 (Microchem Corp.), which has been used extensively in interference lithography. In particular, the single-step soft bake provided excellent process control and reproducibility, and the improved solubility makes it possible to easily remove the resist after template replication. The Futurrex photoresist was deposited by spin-coating onto a 1 mm thick glass slide at 6000 rpm for 40 s, and soft baked on a hot plate for 90 s at 150 °C to achieve a film thickness of approximately 6 μm. An antireflection coating was not required in our experiments because we used transparent glass slides as the substrates.

Samples were exposed using a total laser power of 100 mW before splitting the beam, with the time controlled by a mechanical shutter (VMM-D1, Uniblitz, Inc.). A polarizer positioned under the beam splitter was used to adjust the power of the central beam such that it was equal to the power in each of the side beams, which was approximately 7 mW. The polarization of the expanded incoming beam was maintained parallel to one of the directions from the centre of the beam splitter to a corresponding opening. Exposure times of 0.4 and 1.2 s were used for samples prepared using two different incident angles of 18.5° and 27°. A longer exposure time was required for the samples exposed using the larger 27° incident angle because the area exposed by the three side beams is larger, which leads to a lower exposure intensity. The samples were post-baked at 100 °C for 40 s and then the photoresist was developed in a basic water developer (RD6, Futurrex, Inc.) for 1 min and rinsed in water to remove the regions illuminated with low-intensity light (i.e., below threshold).

3. Results and discussion

In order to demonstrate the flexibility of this tunable beam splitter in fabricating 3D polymer PCs, the negative tone

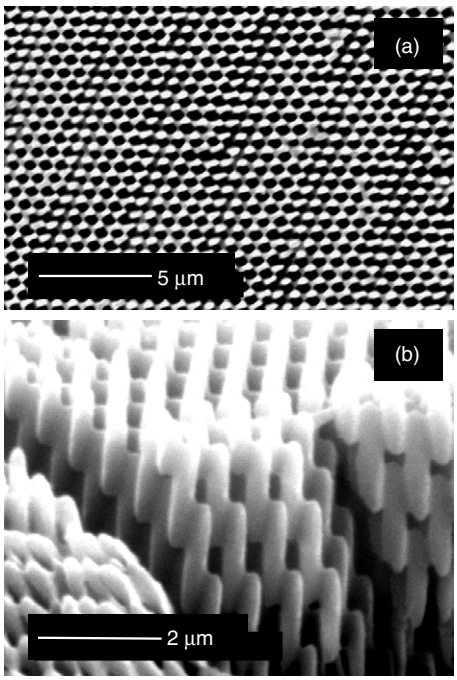

Figure 2. SEM images of a sample fabricated at the incident angle of 18.5°; (a) the in-plane lattice constant is approximately 740 nm as compared to 800 nm predicted theoretically, and (b) the perpendicular lattice constant is approximately 3.7 μm (a–b–c stacking) as compared to 4.3 μm predicted theoretically. SEM images were taken using an accelerating voltage of 20 kV.

photoresist was exposed using two different incident angles of 18.5° and 27° relative to the sample normal. Here, regions of low light intensity correspond to air voids, while regions of high light intensity produce the interconnected 3D polymer structure. The resulting patterns have a hexagonal lattice with in-plane and perpendicular lattice spacing that depends on the angle of incidence; the larger 27° angle will result in features that are more spherical (i.e., with a smaller aspect ratio between the in-plane and perpendicular lattice constants) than those in the 18.5° angle case [15].

Field emission scanning electron microscope (FE-SEM) images of the 3D polymer PCs fabricated using 18.5° and 27° incident angles are shown in figures 2 and 3. The results of these experiments confirm that the tunable beam splitter can be used to create uniform 3D patterns with an open lattice over a large substrate area (>5 mm^2 for this experimental set-up). The in-plane lattice constants measured by imaging the samples at normal incidence (e.g., see figures 2(a) and 3(a)–(c)) for structures fabricated using 18.5° and 27° incident angles are approximately 740 and 500 nm, respectively. The perpendicular lattice constants of the same samples determined from cross-sectional images (e.g., see figures 2(b) and 3(d)) are approximately 3.7 and 1.8 μm (a–b–c stacking) with individual well-defined elliptical features that are approximately 1.7 and 0.8 μm long, respectively. These measured values of the in-plane and perpendicular lattice constant are 5–15% smaller than those predicted theoretically [15], which may be due to shrinkage of the photoresist or a slight sample tilt during FE-SEM measurement. A small chirp is also observed in the crystal structure of these samples. This effect was predicted

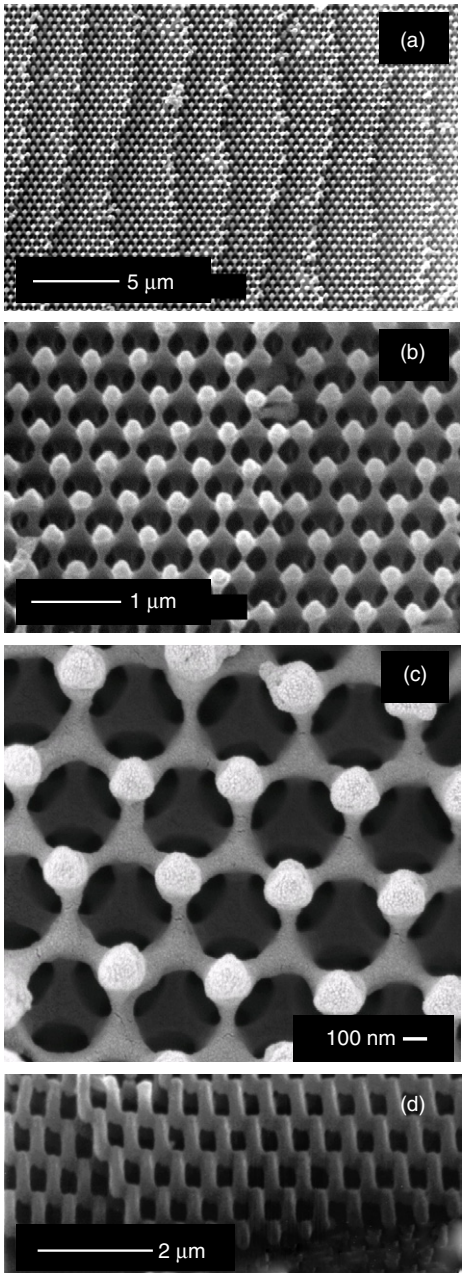

Figure 3. SEM and FE-SEM images of a sample fabricated at the incident angle of 27°; (a) the in-plane lattice constant is approximately 500 nm as compared to 560 nm predicated theoretically; ((b), (c)) higher-magnification images showing a well-defined, open lattice structure; and (d) the perpendicular lattice constant is approximately 1.8 μm (a–b–c stacking) as compared to 2 μm predicted theoretically. SEM and FE-SEM images were taken using accelerating voltages of 20 and 1 kV, respectively.

theoretically by Rumpf *et al* [16], and is due to the optical absorption of the incident beams in the photosensitive polymer, which causes the fill factor and shape of the features to vary slightly with depth from the exposed surface.

The high-magnification FE-SEM image of the 27° incident angle sample shown in figure 3(c) shows the nicely opened lattice, where the second layer of features (i.e., atoms) are displaced from the first layer by one in-plane lattice

constant. It should be noted that the network connecting adjacent features is less than 100 nm in width, which demonstrates that the photoresist used to record these 3D structures has excellent resolution and can be used to fabricate patterns with even smaller periodicity. The open lattice and smooth sidewalls of the features are very important when using such 3D structures as PCs, because any surface roughness will lead to scattering losses that degrade PC performance.

The x–y planes of the 3D lattices fabricated here are equivalent to the (111) plane of the hexagonal crystal structure. However, it is difficult to align perfectly the top surface of the sample to be parallel to the (111) plane during exposure using our prototype beam splitter. Thus, as shown in figure 3(a), we observed clear step edges where the different (111) crystal planes intersect the sample surface. In particular, the step edges are visualized as lighter lines where the atoms of a given plane terminate. As noted in the higher-magnification FE-SEM image of figure 3(b), successive planes differ in height by the z-directed length of the features. Moreover, although not shown, the width of the steps depends on the sample tilt during exposure. The presence of these clear step edges further confirms the integrity of the 3D patterns fabricated using this approach. The above-mentioned misalignment can be eliminated by incorporating a neutral laser beam (e.g., a HeNe laser beam that does not expose the photoresist) that co-propagates with the central non-refracted UV beam. Monitoring the interference pattern created by the reflection from the substrate beam and part of the neutral beam will allow very precise sample tilt compensation prior to exposure.

The as-fabricated low-index-contrast PCs have Γ–X periodicities that will place the corresponding photonic bandgaps in the near infrared (IR) spectral region. In particular, the relationship $\lambda_{\text{gap}} = 2n_{\text{eff}}\, d_{111}$ can be used to estimate the position of the bandgap for this symmetry direction, where n_{eff} is the effective refractive index and d_{111} is the in-plane periodicity of the 3D structure [17]. For the sample fabricated using an incident angle of 27°, we estimate the filling fraction of the photoresist and the separation of the (111) planes to be approximately 0.4 and 590 nm, respectively. Thus, using the photoresist index of refraction of 1.58, the centre of the bandgap will be positioned near 1.50 μm. The centre wavelength can be decreased further into the near IR by increasing the incident angle during sample exposure.

While it was shown previously that such low-index 3D lattice structures will have partial photonic bandgaps [18], recent calculations predict that a complete bandgap can be achieved when the FCC lattice created by interference lithography is inverted with a higher-index material such as Si [19]. This crystal structure can be obtained by interfering beams at an angle of 38.9° inside the polymer, which is larger than the angle of total internal reflection for commercially available photoresists. Thus, coupling elements such as prisms are needed to produce these larger interference angles [17]. The tunable beam splitter demonstrated here can also be used to simplify the adjustments necessary to optimize the coupling angle of the incident beams, which will depend on factors such as the prism geometry and refractive index, the index matching fluid, and the photosensitive polymer.

4. Conclusions

In conclusion, we have presented a new method for fabricating 3D polymer PC structures using a tunable beam splitter that produces four-beam interference patterns from a single incident beam. The flexible design of this beam splitter allows the incident angles and polarization of each of the beams to be adjusted independently, which makes it possible to fabricate structures with different periodicities and space symmetries as well as to optimize the contrast of the high- and low-intensity regions of the interference pattern. Polymer structures fabricated using two different incident angles of 18.5° and 27° had well-defined open lattices with the nm-scale feature resolution required to achieve near IR photonic bandgaps. In addition to direct use as low-index-contrast PCs, such structures could also be used as templates for infiltration of materials with high refractive index.

Acknowledgments

This work was supported by a National Science Foundation Materials Research, Science and Engineering Center for Nanoscale Science under grant DMR-0213623. We would also like to acknowledge the use of the Center for Nanoscale Science Central Facilities Laboratory, and Pennsylvania State University Materials Characterization Laboratory in this research.

References

[1] Shank C V and Schmidt R V 1973 *Appl. Phys. Lett.* **23** 154
[2] Tsang W T and Wang S 1974 *Appl. Phys. Lett.* **24** 196
[3] Chen X, Zaidi S and Brueck S 1996 *J. Vac. Sci. Technol.* B **14** 3339
[4] Grynberg G, Lounis B, Verkerk P, Courtois J and Salomon C 1993 *Phys. Rev. Lett.* **70** 2249
[5] Petsas K, Coates A and Grynberg G 1994 *Phys. Rev.* A **50** 5173
[6] Campbell M, Sharp D N, Harrison M T, Denning R G and Turberfield A J 2000 *Nature* **404** 53
[7] Tondiglia V P, Natarajan L V, Sutherland R L, Tomlin D and Bunning T J 2002 *Adv. Mater.* **14** 187
[8] Yang S, Megens M, Aizenberg J, Wiltzius P, Chaikin P M and Russel W B 2002 *Chem. Mater.* **14** 2831
[9] Sharp D N, Turberfield A J and Denning R G 2003 *Phys. Rev.* B **68** 205102
[10] Ullal C, Maldovan M, Thomas E, Chen G, Han Y-J and Yang S 2004 *Appl. Phys. Lett.* **84** 5434
[11] Cai L, Yang X and Wang Y 2002 *J. Opt. Soc. Am.* A **19** 2238
[12] Yang X, Cai L and Liu Q 2002 *Appl. Opt.* **41** 6894
[13] Su H, Zhong Y, Wang X, Zheng X, Xu J and Wang H 2003 *Phys. Rev.* E **67** 056619
[14] Divliansky I, Shishido A, Khoo I-C, Mayer T, Pena D, Nishimura S, Keating C and Mallouk T 2001 *Appl. Phys. Lett.* **79** 3392
[15] Divliansky I, Mayer T S, Holliday K and Crespi V 2003 *Appl. Phys. Lett.* **82** 1167
[16] Rumpf R and Johnson E 2004 *J. Opt. Soc. Am.* A **21** 1703
[17] Miklyaev Y, Meisel D, Blanco A, von Freymann G, Busch K, Koch W, Enkrich C, Deubel M and Wegener M 2003 *Appl. Phys. Lett.* **82** 1284
[18] Joannopoulos J, Meade R and Winn J 1995 *Photonic Crystals—Molding the Flow of Light* (Princeton, NJ: Princeton University Press)
[19] Meisel D, Wegener M and Busch K 2004 *Phys. Rev.* B **70** 165104